



Published in final edited form as:

Methods. 2012 January ; 56(1): 11–17. doi:10.1016/j.ymeth.2011.09.008.

Biochemical and cell biological analysis of actin in the nematode *Caenorhabditis elegans*

Shoichiro Ono^{a,*} and David Pruyne^b

^aDepartment of Pathology and Department of Cell Biology, Emory University, Atlanta, Georgia 30322, USA

^bDepartment of Cell and Developmental Biology, SUNY Upstate Medical University, Syracuse, NY 13210, USA

Abstract

The nematode *Caenorhabditis elegans* has long been a useful model organism for muscle research. Its body wall muscle is obliquely striated muscle and exhibits structural similarities with vertebrate striated muscle. Actin is the core component of the muscle thin filaments, which are highly ordered in sarcomeric structures in striated muscle. Genetic studies have identified genes that regulate proper organization and function of actin filaments in *C. elegans* muscle, and sequence of the worm genome has revealed a number of conserved candidate genes that may regulate actin. To precisely understand the functions of actin-binding proteins, such genetic and genomic studies need to be complemented by biochemical characterization of these actin-binding proteins *in vitro*. This article describes methods for purification and biochemical characterization of actin from *C. elegans*. Although rabbit muscle actin is commonly used to characterize actin-binding proteins from many eukaryotic organisms, we detect several quantitative differences between *C. elegans* actin and rabbit muscle actin, highlighting that use of actin from an appropriate source is important in some cases. Additionally, we describe probes for cell biological analysis of actin in *C. elegans*.

Keywords

Actin; *C. elegans*; nematodes; purification; polymerization

1. Introduction

Actin is the core component of thin filaments in contractile apparatuses in muscle. In striated muscle, actin filaments are regularly arranged in sarcomeric structures to produce contractile forces. Proper assembly, maintenance, and function of sarcomeric actin filaments are critical for healthy muscle, as defects in sarcomeric actin filaments are associated with a number of cardiac and skeletal muscle diseases in humans [1–6]. Although the sequential events of many steps of sarcomere assembly are well-documented, the molecular mechanism by which sarcomeric actin filaments are assembled and maintained is largely unknown [7–9].

© 2011 Elsevier Inc. All rights reserved.

*Correspondence to: Shoichiro Ono, Department of Pathology, Emory University, 615 Michael Street, Whitehead Research Building, Room 105N, Atlanta, GA 30322, USA, Tel: (404) 727-3916, Fax: (404) 727-8538, sono@emory.edu.

Publisher's Disclaimer: This is a PDF file of an unedited manuscript that has been accepted for publication. As a service to our customers we are providing this early version of the manuscript. The manuscript will undergo copyediting, typesetting, and review of the resulting proof before it is published in its final citable form. Please note that during the production process errors may be discovered which could affect the content, and all legal disclaimers that apply to the journal pertain.

Striated muscle is also present in invertebrates, with a basic sarcomeric organization of contractile proteins very similar to that in vertebrate muscle, and studies in insects and nematodes have provided many of our insights into the mechanisms of sarcomere assembly and function [10].

The body wall muscle of the nematode *Caenorhabditis elegans* is obliquely striated muscle with distinct sarcomeric structures, and has been a powerful model for study of the structure and function of contractile apparatuses in striated muscle (for reviews, [11–13]). In *C. elegans*, actin is 90–94 % identical with human skeletal muscle α -actin [14]. In addition, many actin-binding proteins that regulate assembly and function of vertebrate sarcomeric actin filaments are conserved in *C. elegans* [9]. Genetic approaches have further identified genes that regulate sarcomeric assembly and function in the body wall muscle, and some of them are specifically required for sarcomeric organization of actin filaments [15–17]. Furthermore, sequencing of the genome [18], genome-wide RNA interference studies [19–21], and high-throughput gene expression analyses [22, 23] have revealed additional candidate genes that may regulate sarcomeric actin filaments in *C. elegans*.

To understand the functions of actin regulators, biochemical analysis of their effects on actin dynamics is often important. Since actin sequences are highly conserved among eukaryotic species, rabbit skeletal muscle actin can be used to characterize many *in vitro* properties of actin-binding proteins from *C. elegans*. However, we have found that purified actin from *C. elegans* exhibits several quantitative differences in biochemical properties from rabbit muscle actin [24, 25]. Therefore, use of actin from an appropriate species is important to fully understanding physiologically significant functions of an actin-binding protein. Unfortunately, expression of functional actin requires specific chaperones, and bacterial expression systems are not appropriate. A recently developed baculovirus system for expressing recombinant actin provides a viable alternative for producing single actin isoforms or mutant forms of actin [26]. However, milligram quantities of native actin can be relatively easily purified from *C. elegans* [24]. This article describes methods for purification of *C. elegans* actin and its biochemical and cell biological characterization with updated analysis and additional details.

2. Materials and methods

2.1. Nematode culture

Wild-type *C. elegans* strain N2 was obtained from the *Caenorhabditis* Genetics Center (Minneapolis, MN). Nematodes were generally maintained under standard conditions using nematode growth medium (NGM)-agar plates at 20 °C as described previously [27]. Detailed culture methods for *C. elegans* are described by Stiernagle [28].

For actin preparation, *C. elegans* was grown in liquid culture essentially as described by Stiernagle [28] using *Escherichia coli* NA22 as a food [29]. *E. coli* OP50 can also be used as a food [28]. Detailed methods to prepare required solutions are described by Lewis and Fleming [30] and Stiernagle [28]. Prior to worm culture, *E. coli* was grown in Terrific Broth (12 g/l tryptone, 24 g/l yeast extract, 9.4 g/l K₂HPO₄, 2.2 g/l KH₂PO₄, 0.4 % glycerol) overnight at 37 °C with shaking, harvested by centrifugation at 6000 × g for 10 min, suspended in a small volume of S-basal medium without cholesterol (5.9 g/l NaCl, 1 g/l K₂HPO₄, 6 g/l KH₂PO₄), and kept at 4 °C. We typically grow 4 l of *E. coli* culture and use *E. coli* suspensions within a week. Although *E. coli* pellets or suspensions can be kept frozen, freezing and thawing partially disrupt cells, increasing viscosity of the bacterial suspensions, and making subsequent handling difficult. For preparation of liquid culture, *C. elegans* was grown in 10-cm NGM-agar plates (2–3 plates per 500-ml liquid culture) until they were nearly starved and enriched with L1 larvae. Worms were transferred into 1 l of S-

basal medium with 5 µg/ml cholesterol and divided evenly between two 2-l Erlenmeyer flasks. Each 500 ml culture was supplemented with 5 ml of 1 M potassium citrate (pH 6.0), 5 ml of trace metals solution (1.86 g/l disodium EDTA, 0.69 g/l FeSO₄ • 7 H₂O, 0.2 g/l MnCl₂•4 H₂O, 0.29 g/l ZnSO₄ • 7 H₂O, 0.025 g/l CuSO₄ • 5 H₂O), 1.5 ml of 1 M CaCl₂, 1.5 ml of 1 M MgSO₄ (the complete medium is S medium) and 15–20 ml of *E. coli* suspension, and maintained at room temperature (22–25 °C) with shaking.

Worms were harvested after 5–7 days by centrifugation at 3000 × g for 5 min. They were resuspended in cold 0.1 M NaCl, mixed with equal volume of cold 60 % sucrose, and centrifuged at 3000 × g for 10 min. Live worms that floated to the top of the medium were collected by wide-mouth pipettes. They were then washed twice by suspension in 0.1 M NaCl and pelleting at 3000 × g for 5 min. The worm pellets were kept frozen at –80 °C in 50-ml polypropylene tubes until needed. Typically, 10–15 ml of packed worms is obtained per 500-ml culture, although the yield can be more or less depending on the culture conditions and the amounts of food.

2.2. Purification of actin from *C. elegans*

We reported a method to purify actin from *C. elegans* previously [24]. This method was modified from one originally developed by Harris and colleagues [31] by incorporation of gel filtration chromatography in the presence of a high concentration of Tris, a condition that depolymerizes actin without denaturation and which had been used successfully to purify actin from vertebrate non-muscle tissues [32, 33]. Here, we provide additional details and updated information on the purification of actin from *C. elegans*.

Frozen worm pellets (30–40 ml) were thawed in 2 volumes (1 volume refers to an initial volume of the worm pellets) of a homogenizing buffer (50 mM NaCl, 1 mM EDTA, 1 mM DTT, 1 mM PMSF, 20 mM Tris-HCl, pH 8.0), and homogenized by passing twice through a French pressure cell (Thermo Fisher Scientific, Model FA-031) at 5000 – 8000 lb/in² (360–580 g/cm²) using a Carver Laboratory Press (Model C). The homogenates were centrifuged at 10,000 × g for 10 min, and the pellets (containing myofibrils) were washed twice by resuspension in homogenizing buffer and pelleting at 10,000 × g for 10 min. The washed pellets were extracted with 1 volume of 0.6 M KCl, 5 mM ATP, 5 mM MgCl₂, 0.2 mM EGTA, 1 mM DTT, 1 mM PMSF, 20 mM Tris-HCl, pH 8.0, and centrifuged at 10,000 × g for 10 min, with the high-salt and ATP facilitating extraction of actin filaments by inducing dissociation of actin filaments from myosin. The extraction was repeated once more. The combined supernatants were mixed with 1/20 volume of 10 % Triton X-100 (approximately final 0.5 %, to solubilize membranes) and ultracentrifuged at 100,000 × g for 2 h, with actin filaments recovered in the pellet, and tropomyosin in the supernatant. The supernatant was stored at –80 °C for later purification of tropomyosin as described previously [34], while the pellet was collected using a plastic spatula, and transferred into a Dounce homogenizer containing ice-cold 2 M Tris-HCl, pH 7.0, 1 mM MgCl₂, 0.2 mM ATP, 0.2 mM DTT for homogenization. Homogenized pellet was then ultracentrifuged at 100,000 × g for 1 h to clarify the soluble depolymerized actin.

The actin-containing supernatant was applied to a Sephacryl S-300 gel filtration column. While a manually packed column (1.9 cm in diameter and 90 cm in length, bed volume: 250 ml) was used in our original report, here we used a HiPrep™ 26/60 Sephacryl S-300 pre-packed column (bed volume: 320 ml) (GE Healthcare) attached to an ÄKTA FPLC system (GE Healthcare). The column was equilibrated and eluted with 1 M Tris-HCl, pH 7.0, 0.5 mM MgCl₂, 0.2 mM ATP, 0.2 mM DTT into 50–60 fractions (5–6 ml per fraction) that were analyzed by SDS-PAGE and Coomassie Brilliant Blue R-250 staining for protein composition. A typical elution pattern of proteins from gel filtration chromatography is shown in Fig. 1.

In selection of fractions for further purification, it is important to make sure that actin is well-separated from most of other proteins. For the preparation in Fig. 1, fractions 29–32 (Fig. 1, asterisks) were pooled and dialyzed against G-buffer (2 mM Tris-HCl, pH 8.0, 0.2 mM CaCl₂, 0.2 mM ATP, 0.2 mM DTT) overnight. The appearance of a white insoluble material after dialysis is normal, as reduction in the Tris concentration precipitates contaminating proteins, and therefore the dialysate was clarified by centrifugation at 20,000 × g for 20 min. Actin in the clarified dialysate was then polymerized by adding final 30 mM KCl and 2 mM MgCl₂ and 1 mM ATP for 4 h at room temperature or overnight at 4 °C. F-actin was then pelleted by ultracentrifugation at 100,000 × g for 2 h. For experiments requiring preassembled F-actin, the pellet was resuspended in a small volume of F-buffer (0.1 mM KCl, 2 mM MgCl₂, 0.2 mM ATP, 1 mM DTT, 20 mM HEPES-KOH, pH 7.5), while to obtain G-actin, the pellet was solubilized in G-buffer, dialyzed against G-buffer overnight, and ultracentrifuged at 424,000 × g for 1 h by a Beckman TLA100.3 rotor (100,000 rpm), with G-actin recovered in the supernatant. When removal of actin dimers and oligomers was critical, G-actin was further purified by gel filtration chromatography using a Sephacryl S-300 column that had been equilibrated by G-buffer.

Concentration of F-actin was determined by Pierce® BCA Protein Assay Kit (Thermo Fisher Scientific). Concentration of G-actin was spectrophotometrically determined using an extinction coefficient of 0.63 mg⁻¹ ml cm⁻¹ at 290 nm. This value has been used for rabbit muscle actin, and we verified by SDS-PAGE and densitometry that equivalent concentrations of *Ce*-actin and rabbit actin could be yielded using this value.

2.3. Electrophoresis and Western blot

SDS-PAGE was performed using 12 % acrylamide (acrylamide : bis-acrylamide = 29:1) gels in vertical slab gel systems (16.5 × 14.5 or 11.3 × 10 cm gel) (C. B. S. Scientific).

Total lysates of wild-type *C. elegans* were prepared as described previously [34]. *Ce*-actin was denatured in SDS-lysis buffer (2 % SDS, 80 mM Tris-HCl, 5 % β-mercaptoethanol, 15 % glycerol, 0.05 % bromophenol blue, pH 6.8) at 97 °C for 5 min.

Two-dimensional gel electrophoresis was performed by a combination of isoelectric focusing (IEF) in the first dimension and SDS-PAGE in the second dimension. SDS was removed from the protein samples as described [35]. Proteins were resuspended in IEF sample buffer (8 M urea, 2 % CHAPS, 50 mM DTT, 0.2 % Bio-Lyte 3/10 ampholytes) with brief sonication and applied to pH 4–7 ReadyStrip IPG strips (11 cm gel; Bio-Rad) by passive rehydration. Isoelectric focusing was performed by applying 35,000 V h with a maximum voltage of 8000 V using a Protean IEF Cell (Bio-Rad). The IPG strips were applied to SDS-PAGE for the second dimension and subjected to Coomassie-staining or Western blot as described [36]. The anti-actin monoclonal antibody (C4; ICN Biomedicals) was used as the primary antibody.

2.4. Preparation and characterization of pyrene-labeled *C. elegans* actin

C. elegans G-actin was purified as above to just prior to repolymerization, then dialyzed twice overnight against 2 l cold Ca²⁺ depolymerizing solution (CDS: 10 mM Tris-HCl, pH 8.0, 0.2 mM CaCl₂, 1 mM NaN₃, 0.5 mM ATP, 1 mM DTT), followed by another overnight dialysis against CDS lacking DTT to remove competing sulfhydryl groups. After clarification at 100,000 × g for 15 min, the dialyzed G-actin was labeled with N-(1-pyrene)-iodoacetamide as described previously for rabbit skeletal muscle actin [37] with modifications as described [38]. Specifically, the following were mixed in this order: (1) G-actin plus CDS of sufficient volume to yield 40 μM actin in the final reaction, (2) 1 M MgCl₂ to yield final concentration of 2 mM, (3) dropwise 26 mM (1 mg/mL) N-(1-pyrene)-

iodoacetamide (Molecular Probes® Invitrogen, dissolved in dimethyl sulfoxide) to give a final concentration of 45 μM , and (4) 2.5 M KCl to give a final concentration of 0.1 M. The reaction was incubated for 90 min at 15°C to yield pyrene-labeled F-actin, which required protection from light from this point forward. To obtain pyrene-labeled G-actin, the labeling reaction was pelleted at $100,000 \times g$ for 2.5 h, and the pellet washed twice briefly with ice cold G-buffer (2 mM Tris-HCl, pH 8.0, 0.2 mM CaCl₂, 0.2 mM ATP, 0.2 mM DTT), and soaked for 15 min in the same before disruption of the pellet in a Dounce homogenizer. Disrupted pellet was dialyzed twice overnight against 2 l ice cold G-buffer. For final purification of pyrene-labeled G-actin, the dialysate was clarified at $100,000 \times g$ for 2 h and fractionated on a Sephacryl S-300 column. Actin monomer concentration of pyrene-labeled actin was determined by the following equation [39]:

$$[\text{actin}] \text{ in } \mu\text{M} = ((A_{290}^{\text{actin}} - (0.127 * A_{344}^{\text{actin}})) - (A_{290}^{\text{buffer}} - (0.127 * A_{344}^{\text{buffer}}))) / 0.00249$$

The efficiency of labeling can be calculated based on the amount of pyrene present, which exhibits an extinction coefficient of $22,000 \text{ M}^{-1} \text{ cm}^{-1}$ at 344 nm, with typical efficiency ranging from 75 – 90 % labeled actin, similar to those reported for rabbit actin [39]. For use, this stock was typically diluted with unlabeled actin to 4 – 10 % labeled actin.

3. Results and discussion

3.1. Purification of *C. elegans* actin

C. elegans actin (Ce-actin) that is purified using this method (2.2) is 95–99 % pure (Fig. 2) as determined previously by SDS-PAGE and densitometry and does not contain detectable levels of capping protein or ADF/cofilin [24], which are known to influence the rate of actin polymerization and depolymerization at very low concentrations [40, 41]. In a typical preparation, 5–7 mg of actin is obtained from 30–40 ml of worms, with a small unidentified protein of ~16 kDa (Fig. 2, asterisk) being the only contaminant sometimes detectable in low amounts. Both F- and G-actin are stable on ice for at least two weeks, and G-actin can be snap-frozen in liquid nitrogen and stored at -80°C for longer storage.

With further analysis through two-dimensional gel electrophoresis using isoelectric focusing (IEF) in the first dimension with an immobilized pH gradient, Ce-actin resolves to six distinct spots by Coomassie-blue stain (Fig. 3A). All are recognized by anti-actin monoclonal antibody C4 in Western blots (Fig. 3B), indicating that they are variants of Ce-actin rather than non-actin contaminants of the same molecular weight. In comparison, total worm lysates also exhibit these six actin spots, plus an additional seventh spot of higher pI as recognized by the anti-actin antibody (Fig. 3D). The most basic spot 7 is only detected in total worm lysates, and spot 6 is relatively more intense in total lysates than in purified Ce-actin (Fig. 3B and D). Currently, the molecular identity of these Ce-actin variants is not known, but of the five *C. elegans* actin isoforms (ACT-1 through ACT-5), ACT-5 is predicted to have the highest pI of 5.44, compared to either 5.29 or 5.30 for the others (Table 1). This is due to the presence of His-222 in ACT-5 in replacement of Leu found in other isoforms [42], making it a likely candidate for spots 6 and 7. Also consistent with this, ACT-5 is the only actin isoform known to be restricted to non-muscle tissues [42], whose actin is expected to be lost during the low-salt/ATP-free conditions of the early purification steps.

For the remaining Ce-actins, their predicted pI values differ only slightly (pI 5.29 – 5.30) (Table 1) on account of the substitution of Asp-5 in ACT-2 for Glu in the remaining Ce-actins. This, together with the near identical sequences of the three remaining actins, suggests that the multiplicity of IEF-derived spots likely reflects either post-translational

modifications to Ce-actin, such as N-terminal proteolytic processing, acetylation, or histidine methylation, or artifactual oxidation of Ce-actin during sample processing. Schachat and colleagues have previously reported that *C. elegans* actin behaves as a single electrofocusing species, but for their studies, they used a diffusible pH gradient [43]. However, our results indicate that multiple species can be resolved by an immobilized pH gradient, suggesting this technique might provide a useful tool for analysis of post-translational modifications of actin in *C. elegans*.

3.2. Biochemical properties of *C. elegans* actin

C. elegans actins are >90 % identical in amino acid sequences to vertebrate skeletal muscle α -actin, and the crystal structure of Ce-actin (Protein Data Bank accession number 1D4X) shows no major differences from that of rabbit muscle α -actin [44]. Nonetheless, biochemical examination of the properties of Ce-actin revealed several quantitative differences from those of rabbit muscle actin. The critical concentration of Ce-actin is ~ 0.5 μM , which is slightly higher than that of rabbit muscle actin (~ 0.3 μM) under the same experimental conditions [24]. Further, the kinetics of spontaneous polymerization from G-actin are slightly slower for Ce-actin than for rabbit muscle actin [24], and Ce-actin exchanges actin-bound ATP ~ 2 -fold faster than rabbit muscle actin [25].

We have noticed the most significant differences between Ce-actin and rabbit muscle actin in their interactions with UNC-60B, a muscle-specific actin depolymerizing factor (ADF)/cofilin isoform in *C. elegans* [36, 45, 46]. UNC-60B severs rabbit muscle actin filaments more efficiently than Ce-actin filaments [25, 36], but enhances dissociation of actin monomers more efficiently from Ce-actin filaments than from rabbit muscle actin filaments [24, 25], potentially indicating the function of UNC-60B in enhancing disassembly of Ce-actin filaments is more likely to be by the latter mechanism. However, a mutation that impairs filament severing by UNC-60B causes severe disorganization of actin filaments in the body wall muscle [36, 47, 48], indicating that severing is in fact critical to its *in vivo* function. Resolving these biochemical and genetic findings, we found that *in vitro* severing of actin filaments by UNC-60B is enhanced by a co-factor, actin-interacting protein 1 (AIP1) [49–52], and in support of the *in vivo* importance of this function, mutations in the *C. elegans* AIP1 genes (*unc-78* and *aipl-1*) cause severe disorganization of muscle actin filaments [53, 54]. Thus, while biochemical studies of the effects of UNC-60B on rabbit muscle actin filaments highlighted its ability to sever filaments, analysis of its effects on Ce-actin filaments more accurately reflect the importance of the AIP1 proteins (UNC-78 and AIPL-1) in enhancing its relatively weak activity toward the endogenous substrate, and suggest that the native actin is more likely to be a useful tool in characterizing the biochemistry of actin/UNC-60B/AIP1 interactions.

3.3. Biochemical methods to analyze dynamic properties of *C. elegans* actin

Biochemical techniques that have been used to characterize interactions between actin and actin regulatory proteins from other species are readily translated to study Ce-actin [55, 56]. F-actin co-sedimentation assays by ultracentrifugation have been used to examine the binding of proteins to *C. elegans* F-actin [24, 25, 34, 36, 57], as well as to determine the effects of a protein on disassembly of F-actin into G-actin or short actin oligomers [50]. Monomeric Ce-actin binds to and inhibits bovine DNase I in a similar manner as rabbit muscle actin [24], making DNase I inhibition assays useful to quantify G-actin concentrations [24, 36]. Ce-actin binds to 1,*N*⁶-etheno ATP (Invitrogen), a fluorescent analog of ATP, allowing monitoring of the rate of exchange of actin-bound nucleotide [25]. Further, the conserved nature of actin filaments allows for such basic techniques as measuring turbidity (absorbance at 310 nm) using a spectrophotometer [24, 36] or light

scattering at 400 nm using a fluorescence spectrophotometer [25] for monitoring kinetics of polymerization or depolymerization of unlabeled actin.

Fluorescently labeled actin is another tool translatable to study Ce-actin. Pyrene, which in the form of N-(1-pyrene)-iodoacetamide will attach covalently to actin Cys-374, has the property of undergoing a strong increase in fluorescence upon polymerization without altering polymerization properties of actin [37, 39]. Since Ce-actin co-polymerizes with rabbit muscle actin, pyrene-labeled rabbit muscle actin can be used as a fluorescent probe to monitor actin polymerization and depolymerization. As examples, we have used pyrene-labeled rabbit muscle G-actin to quantify relative numbers of exposed barbed ends of Ce-actin filaments [25, 36], and used co-polymers of unlabeled Ce-actin (90 %) and pyrene-labeled rabbit muscle actin (10 %) to monitor kinetics of actin depolymerization [58]. More recently, we have confirmed that Ce-actin can be directly labeled with pyrene by essentially the same method for rabbit muscle actin, and that pyrene-labeled Ce-actin fluoresces over eight-fold brighter in the F-actin form compared to G-actin, and behaves qualitatively similar to rabbit muscle pyrene-actin. For example, a mixture of unlabeled *C. elegans* G-actin and pyrene-labeled Ce-G-actin diluted into polymerizing buffer shows little increase in fluorescence at early time points, reflecting the inefficiency of spontaneous filament nucleation for pure Ce-actin, but in the presence of an actin filament nucleator, such as recombinant fragments of the worm formin CYK-1, exhibits robust and rapid polymerization similar to rabbit muscle actin [59] (Fig. 4). Similarly, pyrene-actin can monitor effects of factors on disassembly, where slowing of depolymerization might reflect capping of barbed ends, or acceleration of depolymerization might reflect severing. A perhaps more significant use for pyrene-labeled Ce-actin is to monitor binding of other proteins independently of their effects on polymerization or depolymerization. For example, binding of *C. elegans* gelsolin-like protein 1 (GSNL-1) to G-actin enhances pyrene fluorescence [60], while binding of ADF/cofilin to pyrene-labeled F-actin quenches fluorescence even in the absence of filament disassembly ([61]; S. O., unpublished data). Such effects can be useful to determine affinity or rate constants for association and dissociation between Ce-actin and the protein of interest. Also, they show the importance of evaluating both polymerization-dependent and -independent changes in pyrene fluorescence need to be carefully evaluated for each experiment when a new actin-binding protein is investigated.

Ce-actin binds to actin-binding proteins from other species, potentially making such proteins useful for biochemical characterization of Ce-actin particularly when they are easier to obtain than the endogenous homologs and when precise details of their interactions with Ce-actin are not critical. For example, chicken capping protein caps the barbed ends of Ce-actin filaments with high affinity and is useful to selectively block polymerization and depolymerization from the barbed ends in *in vitro* assays. We have used chicken capping protein to determine depolymerization of Ce-actin from the pointed ends by ADF/cofilin [25, 58]. Capping protein is a heterodimer of α and β subunits and simultaneous expression of both subunits in *E. coli* is a key to producing properly folded capping protein [62], something readily accomplished for chicken capping protein using the bacterial expression vector available from Addgene (Plasmid # 13451). Human gelsolin segment-1 binds to Ce-actin to prevent polymerization and has been used in crystallographic analysis of the structure of Ce-actin [44]. The binding of bovine DNase I to monomeric Ce-actin can be used to quantify G-actin concentrations by DNase I inhibition assays, as described above [24].

Ce-actin also behaves similarly to rabbit muscle actin with respect to several commonly used actin-binding small molecules, including latrunculin A and phalloidin. Latrunculin A binds to G-actin and prevents polymerization but does not actively enhance

depolymerization. Therefore, we have used latrunculin A to determine effects of ADF/cofilins on Ce-actin depolymerization *in vitro* [25, 58]. Conversely, phalloidin binds to actin filaments and prevents depolymerization. Although we have not used phalloidin in *in vitro* studies, fluorescently labeled phalloidin labels Ce-actin filaments in fixed worms [53], and it is expected to be useful when Ce-actin filaments need to be stabilized, or when Ce-actin filaments need to be visualized by fluorescently labeled phalloidin.

3.4. Cell biological analysis of actin in *C. elegans*

The highly conserved sequences of Ce-actin isoforms compared to those of other organisms allow researchers to use several commonly used actin probes for cell biological analysis of actin in *C. elegans*. We have confirmed that three commercially available anti-actin antibodies specifically recognize actin in *C. elegans*. Two of them are useful for immunofluorescent staining of actin in fixed *C. elegans* worms and embryos. Mouse monoclonal anti-actin antibody C4 (MP Biomedicals; Millipore) [63] specifically recognizes actin in *C. elegans* and can be used for both Western blot and immunohistochemistry [36, 49, 53]. Likewise, rabbit polyclonal anti-actin antibody from Cytoskeleton, Inc. (catalog number: AAN01) specifically recognizes actin in *C. elegans* and can be used for both Western blot and immunohistochemistry [46]. For immunofluorescent staining of worms and embryos, fixation by cold methanol (-20°C , 5 min) [34, 54, 64], 4 % paraformaldehyde [36, 53, 64], or the whole-mount procedure as reported by Finney and Ruvkun [65] are all compatible with these antibodies. Availability of two antibodies from different host species is extremely useful when samples need to be simultaneously stained with anti-actin and other antibodies made in different species. Mouse monoclonal anti-actin antibody JLA20 (Developmental Studies Hybridoma Bank) [66] also specifically recognizes actin in *C. elegans* lysates on Western blot (our unpublished data), but we have not been successful in using this antibody for immunohistochemistry. JLA20 is IgM, and perhaps, it may not easily penetrate into fixed tissues.

As mentioned, fluorescently labeled phalloidin is another useful probe for visualizing Ce-actin filaments microscopically. We routinely use tetramethylrhodamine-phalloidin (Sigma-Aldrich, catalog number P1951) to determine actin filament organization in body wall muscle and other tissues in worms using a method as described previously [53]. In this method, worms are fixed with 4 % paraformaldehyde in $1 \times$ cytoskeleton buffer (10 mM MES-KOH, pH 6.1, 138 mM KCl, 3 mM MgCl_2 , 2 mM EGTA) containing 0.32 M sucrose, followed by permeabilization with acetone at -20°C for 5 min, washing with PBS containing 0.5 % Triton X-100 and 30 mM glycine for 10 min, and staining with 0.2 $\mu\text{g/ml}$ tetramethylrhodamine-phalloidin in the same buffer for 30 min. A common source of failure to stain is poor permeabilization of worms with cold acetone. This problem is circumvented by ensuring fixative is removed as completely as possible before adding acetone, and by loosening worm pellets by tapping to avoid clumping of worms in acetone. Also notable, fixation by cold methanol is not compatible with phalloidin staining and should be avoided, as methanol partially denatures actin filaments and drastically changes the pattern of phalloidin staining.

Unfortunately, the availability of probes for live imaging of actin filaments in *C. elegans* muscle lags behind other systems. However, *C. elegans* has a transparent body, and its sarcomeric structures can be observed in live animals without dissection, indicating that it could be a powerful system to study *in vivo* actin dynamics by using appropriate live probes for actin filaments and imaging techniques. In particular, GFP-actin has been widely used for characterization of live dynamics of actin filaments in a variety of cell types including striated muscle [67–70], and GFP-tagged *C. elegans* ACT-2 has been shown to incorporate into sarcomeric thin filaments in body wall muscle [71]. We have also preliminarily observed that GFP-ACT-4 similarly incorporates into sarcomeric thin filaments in body wall

muscle (S. Ono, unpublished data). These may be potentially useful probes for imaging the live dynamics of actin in *C. elegans* muscle *in vivo*. In addition, small actin-binding domains from several actin-binding proteins have also been used as live probes for actin filaments in non-muscle systems, and some of them might be of use for muscle research in *C. elegans*. For example, Lifeact [72], a 17-amino-acid actin-binding peptide from yeast Abp140p, has recently been used to visualize actin filaments in live cells. Lifeact binds to actin filaments with high specificity and low affinity without interfering with actin dynamics [72], and GFP-Lifeact has been shown to localize to sarcomeric thin filaments in mouse heart [73]. However, Lifeact does not bind to ADF/cofilin-decorated actin filaments [74], pointing to the importance of carefully evaluating such probes for their limitations. With the availability of tools such as these, the analysis of actin dynamics in the living worm muscle represents one of the areas of research ripest for expansion.

3.5. Conclusion

It is through combination of biochemistry, genetics, and cell biology that our understanding of the mechanisms of assembly and maintenance of actin cytoskeletal structures is most complete. *C. elegans* is one of the most useful model organisms for combining multiple technical approaches. Although many of the mechanisms of cytoskeletal regulation are expected to be conserved between *C. elegans* and other species, comparative studies have shown that differences do exist in actin/actin-binding protein interactions, and therefore biochemical functions of actin-binding proteins ought to be carefully characterized using actin of the appropriate species. For *C. elegans*, the ease with which its actin can be obtained and its compatibility with a wide range of biochemical techniques already available make this organism an attractive model system for studying the actin cytoskeleton.

Acknowledgments

The *C. elegans* strain was provided by the *Caenorhabditis* Genetics Center, which is funded by the NIH National Center for Research Resources. This work was supported by NIH grant AR48615 to S. O. and by the American Heart Association to D. P.

References

1. Clarke NF. *Adv. Exp. Med. Biol.* 2008; 642:40–54. [PubMed: 19181092]
2. Clarkson E, Costa CF, Machesky LM. *J. Pathol.* 2004; 204:407–417. [PubMed: 15495263]
3. Ilkovski B. *Adv. Exp. Med. Biol.* 2008; 642:55–65. [PubMed: 19181093]
4. North KN, Laing NG. *Adv. Exp. Med. Biol.* 2008; 642:15–27. [PubMed: 19181090]
5. Tubridy N, Fontaine B, Eymard B. *Curr. Opin. Neurol.* 2001; 14:575–582. [PubMed: 11562568]
6. Michele DE, Metzger JM. *J. Mol. Med.* 2000; 78:543–553. [PubMed: 11199327]
7. Sanger JW, Wang J, Fan Y, White J, Sanger JM. *J. Biomed. Biotechnol.* 2010; 2010:858606. [PubMed: 20625425]
8. Littlefield R, Fowler VM. *Annu. Rev. Cell Dev. Biol.* 1998; 14:487–525. [PubMed: 9891791]
9. Ono S. *Cytoskeleton (Hoboken)*. 2010; 67:677–692. [PubMed: 20737540]
10. Hooper SL, Hobbs KH, Thuma JB. *Prog. Neurobiol.* 2008; 86:72–127. [PubMed: 18616971]
11. Moerman, DG.; Fire, A. *C. elegans* II. Riddle, DL.; Blumenthal, T.; Meyer, BJ.; Priess, JR., editors. Plainview, NY: Cold Spring Harbor Laboratory Press; 1997. p. 417-470.
12. Waterston, RH. *The Nematode C. elegans*. Wood, WB., editor. Cold Spring Harbor Laboratory; 1988. p. 281-335.
13. Moerman DG, Williams BD. *WormBook*. 2006:1–16. [PubMed: 18050483]
14. Landel CP, Krause M, Waterston RH, Hirsh D. *J. Mol. Biol.* 1984; 180:497–513. [PubMed: 6098683]
15. Williams BD, Waterston RH. *J. Cell Biol.* 1994; 124:475–490. [PubMed: 8106547]

16. Waterston RH, Thomson JN, Brenner S. *Dev. Biol.* 1980; 77:271–302. [PubMed: 7190524]
17. Zengel JM, Epstein HF. *Cell Motil.* 1980; 1:73–97. [PubMed: 7348600]
18. The *C. elegans* Sequencing Consortium. *Science.* 1998; 282:2012–2018. [PubMed: 9851916]
19. Kamath RS, Fraser AG, Dong Y, Poulin G, Durbin R, Gotta M, Kanapin A, Le Bot N, Moreno S, Sohrmann M, Welchman DP, Zipperlen P, Ahringer J. *Nature.* 2003; 421:231–237. [PubMed: 12529635]
20. Simmer F, Moorman C, Van Der Linden AM, Kuijk E, Van Den Berghe PV, Kamath R, Fraser AG, Ahringer J, Plasterk RH. *PLoS Biol.* 2003; 1:E12. [PubMed: 14551910]
21. Rual JF, Ceron J, Koreth J, Hao T, Nicot AS, Hirozane-Kishikawa T, Vandenhaute J, Orkin SH, Hill DE, van den Heuvel S, Vidal M. *Genome Res.* 2004; 14:2162–2168. [PubMed: 15489339]
22. Fox RM, Watson JD, Von Stetina SE, McDermott J, Brodigan TM, Fukushige T, Krause M, Miller DM. *Genome Biol.* 2007; 8:R188. [PubMed: 17848203]
23. Dupuy D, Bertin N, Hidalgo CA, Venkatesan K, Tu D, Lee D, Rosenberg J, Svrikapa N, Blanc A, Carnec A, Carvunis AR, Pulak R, Shingles J, Reece-Hoyes J, Hunt-Newbury R, Viveiros R, Mohler WA, Tasan M, Roth FP, Le Peuch C, Hope IA, Johnsen R, Moerman DG, Barabasi AL, Baillie D, Vidal M. *Nat. Biotechnol.* 2007; 25:663–668. [PubMed: 17486083]
24. Ono S. *Cell Motil. Cytoskeleton.* 1999; 43:128–136. [PubMed: 10379837]
25. Yamashiro S, Mohri K, Ono S. *Biochemistry.* 2005; 44:14238–14247. [PubMed: 16245940]
26. Joel PB, Fagnant PM, Trybus KM. *Biochemistry.* 2004; 43:11554–11559. [PubMed: 15350141]
27. Brenner S. *Genetics.* 1974; 77:71–94. [PubMed: 4366476]
28. Stiernagle T. *WormBook.* 2006:1–11. [PubMed: 18050451]
29. Schachat F, Garcea RL, Epstein HF. *Cell.* 1978; 15:405–411. [PubMed: 82486]
30. Lewis JA, Fleming JT. *Methods Cell Biol.* 1995; 48:3–29. [PubMed: 8531730]
31. Harris HE, Tso MY, Epstein HF. *Biochemistry.* 1977; 16:859–865. [PubMed: 139159]
32. Schafer DA, Jennings PB, Cooper JA. *Cell Motil. Cytoskeleton.* 1998; 39:166–171. [PubMed: 9484958]
33. Pinder JC, Sleep JA, Bennett PM, Gratzner WB. *Anal. Biochem.* 1995; 225:291–295. [PubMed: 7762794]
34. Ono S, Ono K. *J. Cell Biol.* 2002; 156:1065–1076. [PubMed: 11901171]
35. Wessel D, Flugge UI. *Anal. Biochem.* 1984; 138:141–143. [PubMed: 6731838]
36. Ono S, Baillie DL, Benian GM. *J. Cell Biol.* 1999; 145:491–502. [PubMed: 10225951]
37. Kouyama T, Mihashi K. *Eur. J. Biochem.* 1981; 114:33–38. [PubMed: 7011802]
38. Northrop J, Weber A, Mooseker MS, Franzini-Armstrong C, Bishop MF, DUBYAK GR, Tucker M, Walsh TP. *J. Biol. Chem.* 1986; 261:9274–9281. [PubMed: 3087992]
39. Cooper JA, Walker SB, Pollard TD. *J. Muscle Res. Cell Motil.* 1983; 4:253–262. [PubMed: 6863518]
40. Casella JF, Barron-Casella EA, Torres MA. *Cell Motil. Cytoskeleton.* 1995; 30:164–170. [PubMed: 7606809]
41. Du J, Frieden C. *Biochemistry.* 1998; 37:13276–13284. [PubMed: 9748335]
42. MacQueen AJ, Baggett JJ, Perumov N, Bauer RA, Januszewski T, Schrieffer L, Waddle JA. *Mol. Biol. Cell.* 2005; 16:3247–3259. [PubMed: 15872090]
43. Schachat FH, Harris HE, Epstein HF. *Biochim. Biophys. Acta.* 1977; 493:304–309. [PubMed: 889873]
44. Vorobiev S, Strokopytov B, Drubin DG, Frieden C, Ono S, Condeelis J, Rubenstein PA, Almo SC. *Proc. Natl. Acad. Sci. USA.* 2003; 100:5760–5765. [PubMed: 12732734]
45. McKim KS, Matheson C, Marra MA, Wakarchuk MF, Baillie DL. *Mol. Gen. Genet.* 1994; 242:346–357. [PubMed: 8107682]
46. Ono K, Parast M, Alberico C, Benian GM, Ono S. *J. Cell Sci.* 2003; 116:2073–2085. [PubMed: 12679387]
47. Ono K, Yamashiro S, Ono S. *J. Cell Sci.* 2008; 121:2662–2670. [PubMed: 18653537]
48. Ono S, McGough A, Pope BJ, Tolbert VT, Bui A, Pohl J, Benian GM, Gernert KM, Weeds AG. *J. Biol. Chem.* 2001; 276:5952–5958. [PubMed: 11050090]

49. Mohri K, Ono K, Yu R, Yamashiro S, Ono S. *Mol. Biol. Cell.* 2006; 17:2190–2199. [PubMed: 16525019]
50. Mohri K, Ono S. *J. Cell Sci.* 2003; 116:4107–4118. [PubMed: 12953066]
51. Mohri K, Vorobiev S, Fedorov AA, Almo SC, Ono S. *J. Biol. Chem.* 2004; 279:31697–31707. [PubMed: 15150269]
52. Ono S, Mohri K, Ono K. *J. Biol. Chem.* 2004; 279:14207–14212. [PubMed: 14742433]
53. Ono S. *J. Cell Biol.* 2001; 152:1313–1319. [PubMed: 11257131]
54. Ono S, Nomura K, Hitosugi S, Tu DK, Lee JA, Baillie DL, Ono K. *Mol. Biol. Cell.* 2011; 22:2258–2269. [PubMed: 21551072]
55. Hertzog M, Carlier MF. *Curr. Protoc. Cell Biol.* 2005; Chapter 13(Unit 13 16)
56. Pollard TD, Cooper JA. *Methods Enzymol.* 1982; 85:211–233. [PubMed: 6889670]
57. Yamashiro S, Gimona M, Ono S. *J. Cell Sci.* 2007; 120:3022–3033. [PubMed: 17684058]
58. Yamashiro S, Cox EA, Baillie DL, Hardin JD, Ono S. *J. Cell Sci.* 2008; 121:3867–3877. [PubMed: 18984629]
59. Amin NM, Hu K, Pruyne D, Terzic D, Bretscher A, Liu J. *Development.* 2007; 134:19–29. [PubMed: 17138663]
60. Kilaavuniemi T, Yamashiro S, Ono S. *J. Biol. Chem.* 2008; 283:26071–26080. [PubMed: 18640981]
61. Nishida E, Maekawa S, Sakai H. *Biochemistry.* 1984; 23:5307–5313. [PubMed: 6509022]
62. Soeno Y, Abe H, Kimura S, Maruyama K, Obinata T. *J. Muscle Res. Cell Motil.* 1998; 19:639–646. [PubMed: 9742448]
63. Lessard JL. *Cell Motil. Cytoskeleton.* 1988; 10:349–362. [PubMed: 2460261]
64. Ono K, Yu R, Ono S. *Dev. Dyn.* 2007; 236:1093–1105. [PubMed: 17326220]
65. Finney M, Ruvkun G. *Cell.* 1990; 63:895–905. [PubMed: 2257628]
66. Lin JJ. *Proc. Natl. Acad. Sci. USA.* 1981; 78:2335–2339. [PubMed: 7017730]
67. Skwarek-Maruszewska A, Hotulainen P, Mattila PK, Lappalainen P. *J. Cell Sci.* 2009; 122:2119–2126. [PubMed: 19470580]
68. Wang J, Shaner N, Mittal B, Zhou Q, Chen J, Sanger JM, Sanger JW. *Cell Motil. Cytoskeleton.* 2005; 61:34–48. [PubMed: 15810059]
69. Bai J, Hartwig JH, Perrimon N. *Dev. Cell.* 2007; 13:828–842. [PubMed: 18061565]
70. Sanger JW, Wang J, Holloway B, Du A, Sanger JM. *Cell Motil. Cytoskeleton.* 2009; 66:556–566. [PubMed: 19382198]
71. Willis JH, Munro E, Lyczak R, Bowerman B. *Mol. Biol. Cell.* 2006; 17:1051–1064. [PubMed: 16407404]
72. Riedl J, Crevenna AH, Kessenbrock K, Yu JH, Neukirchen D, Bista M, Bradke F, Jenne D, Holak TA, Werb Z, Sixt M, Wedlich-Soldner R. *Nat. Methods.* 2008; 5:605–607. [PubMed: 18536722]
73. Riedl J, Flynn KC, Raducanu A, Gartner F, Beck G, Bosl M, Bradke F, Massberg S, Aszodi A, Sixt M, Wedlich-Soldner R. *Nat. Methods.* 2010; 7:168–169. [PubMed: 20195247]
74. Munsie LN, Caron N, Desmond CR, Truant R. *Nat. Methods.* 2009; 6:317. [PubMed: 19404250]
75. Gasteiger E, Gattiker A, Hoogland C, Ivanyi I, Appel RD, Bairoch A. *Nucleic Acids Res.* 2003; 31:3784–3788. [PubMed: 12824418]

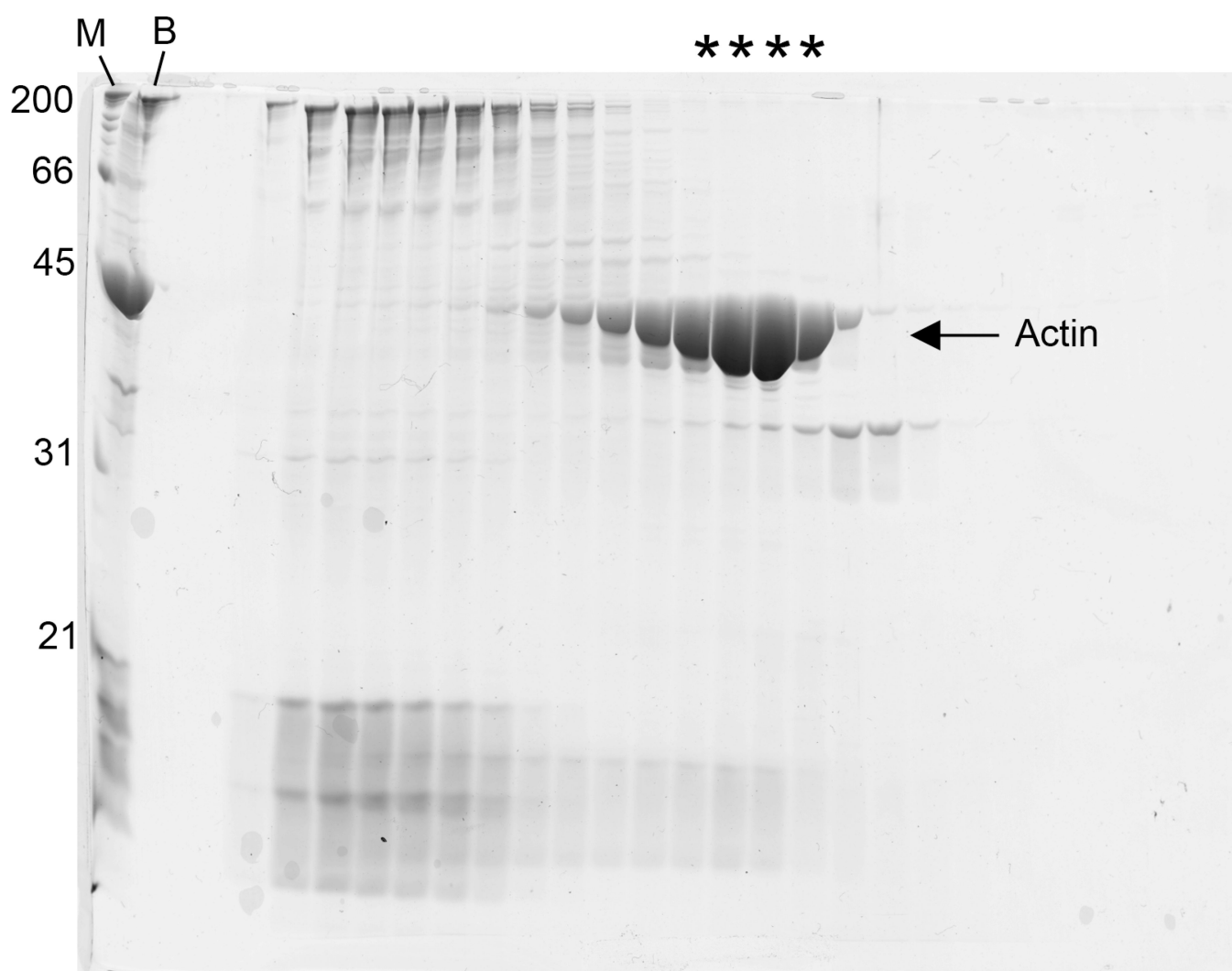


Fig. 1. Gel filtration chromatography of actin in the presence of 1 M Tris. Crude actin after depolymerization by 2 M Tris (lane B) was applied to Sephacryl S-300 gel filtration chromatography. The eluates were fractionated into ~60 fractions, and fractions 16 – 40 were examined by SDS-PAGE and Coomassie staining. Molecular weight markers were applied to lane M (note that the markers are disturbed due to the presence of high concentrations of Tris in other samples) and indicated on the left of the gel. Asterisks indicate 4 fractions (fractions 29–32), which were pooled for the subsequent dialysis against G-buffer.

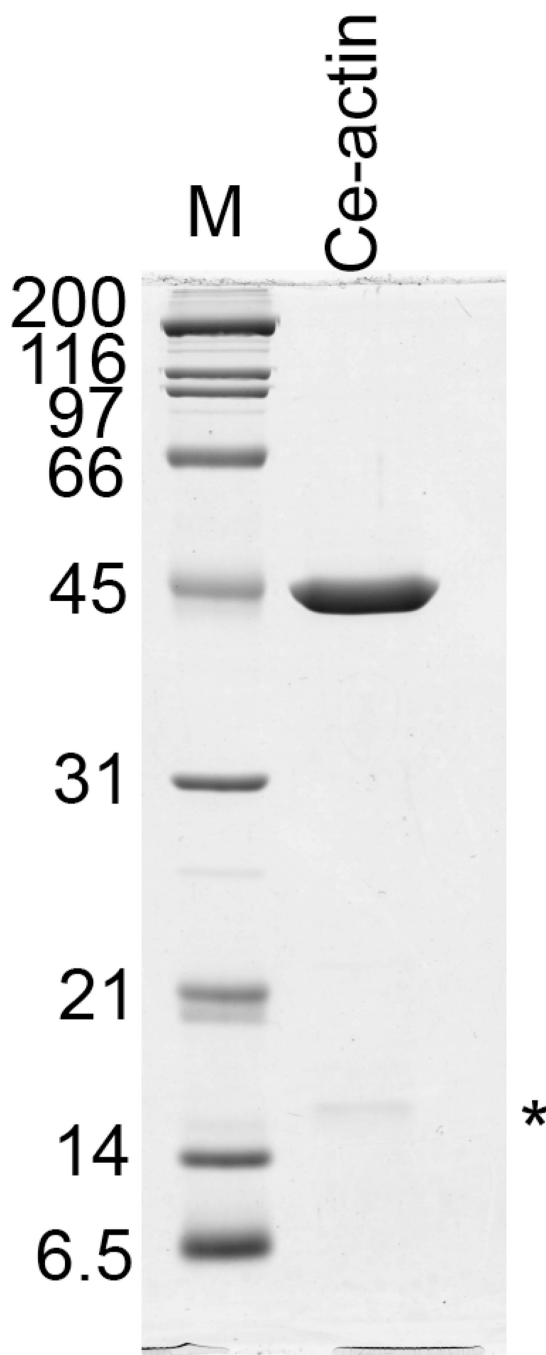


Fig. 2. The final preparation of Ce-actin. Six micrograms of purified Ce-actin were examined by SDS-PAGE and Coomassie staining. An asterisk indicates a 16-kDa protein that is typically present in a Ce-actin preparation [24]. Molecular identity of this protein is currently unknown. Molecular weight markers were applied to lane M and indicated on the left of the gel.

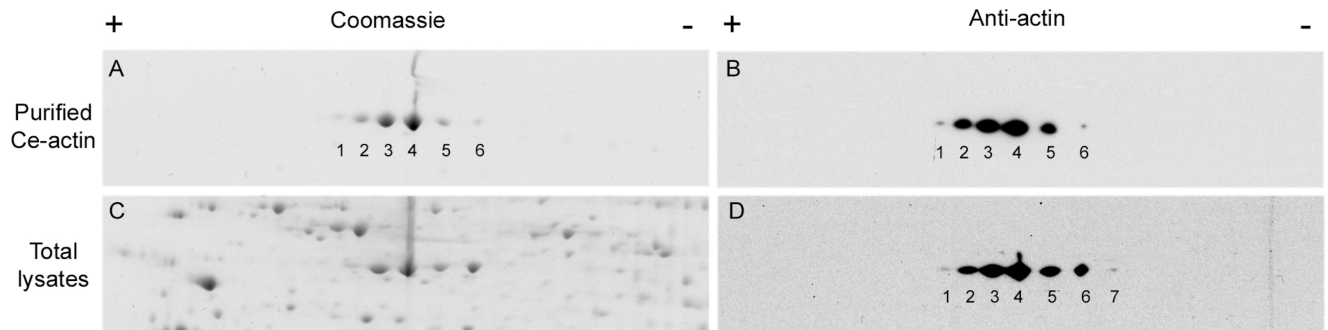


Fig. 3.

Analysis of Ce-actin by two-dimensional electrophoresis. Purified Ce-actin (1.7 μg in panel A and 0.17 μg in panel B) or total worm lysates (100 μg protein in panel C and 10 μg protein in panel D) were resolved by isoelectric focusing in the first (horizontal) dimension and SDS-PAGE in the second (vertical) dimension and stained with Coomassie blue (A and C) or subjected to Western blot with anti-actin antibody C4 (B and D). Acidic side (+) is on the left.

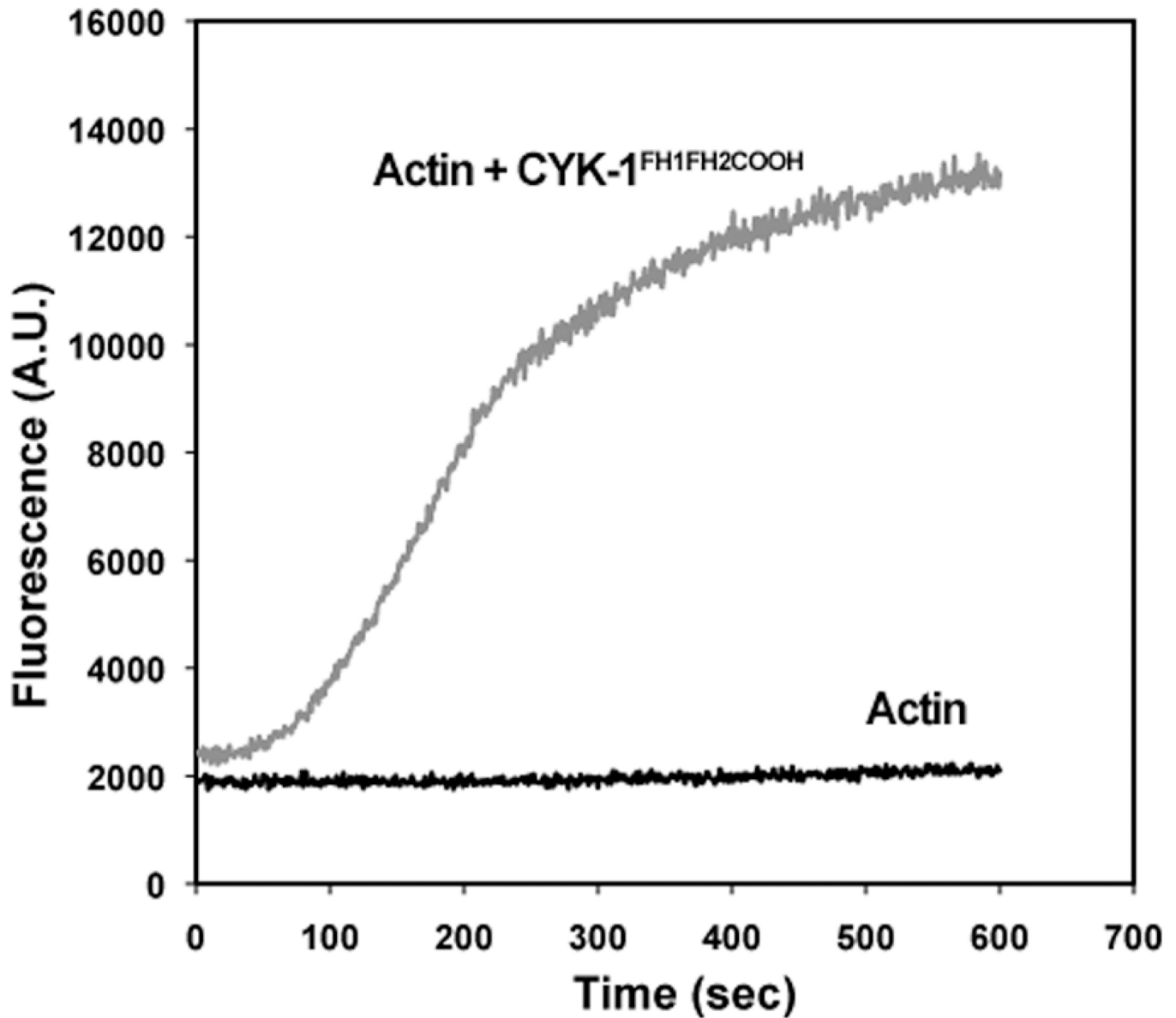


Fig. 4.

Pyrene actin polymerization. Purified pyrene-labeled Ce-actin was mixed with unlabeled protein to yield 4 % labeled actin and diluted with either formin storage buffer (50 mM KCl, 20 mM HEPES, pH 7.5, 5 % glycerol, 1 mM DTT) (bottom black curve) or an equal volume of buffer containing a recombinant C-terminal fragment of the worm formin CYK-1, including the FH1 and FH2 domains (top gray curve), resulting in final concentrations of 2.5 μ M Ce-actin and (if present) 100 nM CYK-1. Actin polymerization was induced by addition of 10 \times polymerization buffer (0.5 M KCl, 20 mM MgCl₂, 1 mM ATP) at time 0, and monitored as increase in pyrene fluorescence (excitation at 365 nm and emission at 407 nm).

Table 1

Comparison of estimated isoelectric points (pI) of actin proteins

Actin protein	Amino acids ^a	pI ^b
Human skeletal muscle α -actin (ACTA1)	377	5.23
Human cardiac muscle α -actin (ACTC1)	377	5.23
Human smooth muscle α -actin (ACTA2)	377	5.24
Human cytoplasmic β -actin (ACTB)	375	5.29
Human cytoplasmic γ -actin (ACTG1)	375	5.31
Human enteric γ -actin (ACTG2)	376	5.31
<i>C. elegans</i> ACT-1	376	5.30
<i>C. elegans</i> ACT-2	376	5.29
<i>C. elegans</i> ACT-3	376	5.30
<i>C. elegans</i> ACT-4	376	5.30
<i>C. elegans</i> ACT-5	375	5.44

^aNumbers of amino acids are based on complete sequences from cDNAs. N-terminal processing in mature actin is not considered.

^bpI values were estimated by the ProtParam Tool on the ExPASy Server [75].